Horizontal Reactive Distillation for Multicomponent Chiral Resolution

Patrick H. Au-Yeung
Engineering and Process Science, Core R&D, The Dow Chemical Company, Midland, MI, 48667

Sol M. Resnick
Biotechnology R&D, The Dow Chemical Company, San Diego, CA, 92121

Paul M. Witt and Timothy C. Frank
Engineering and Process Science, Core R&D, The Dow Chemical Company, Midland, MI, 48667

Felipe A. Donate
Performance Chemicals R&D, The Dow Chemical Company, Midland, MI, 48667

Lanny A. Robbins
Core R&D, The Dow Chemical Company, Midland, MI, 48667

DOI 10.1002/aic.14138
Published online May 28, 2013 in Wiley Online Library (wileyonlinelibrary.com)

A novel horizontal reactive distillation apparatus and a new overall process scheme are proposed for continuous multicomponent chiral resolution via reversible enantioselective acylation of a chiral (racemic) substrate by a chiral (racemic) acyl donor. The process enables simultaneous production of up to four enantiomers with enhanced chiral purity. Kinetic studies, miniplant experiments, and process simulation results are described for a model lipase-catalyzed reaction: (R)-enantioselective transesterification of (R,S)-1-n-butoxy-2-propanol with (R,S)-1-methoxy-2-acetoxypropane to produce (R)-1-n-butoxy-2-acetoxypropane, (R)-1-methoxy-2-propanol, and the two unreacted (S)-enantiomers of the (R,S)-reagents. A horizontal, compartmentalized reactive distillation vessel is specified instead of a conventional reactive distillation column to provide longer liquid-phase residence time needed for adequate conversion. Low vapor-traffic pressure drop allows operation under vacuum at reduced temperatures for good enzyme stability and enantioselectivity. The general technology has potential as a means to producing a wide range of chiral synthons used in asymmetric syntheses of chiral pharmaceuticals and other biologically active products. © 2013 American Institute of Chemical Engineers *AIChE J*, 59: 2603–2620, 2013
Keywords: enantiomer, acylation, glycol ether, transesterification, process

Introduction

New process options are needed to facilitate the selective manufacture of chiral products including pharmaceuticals, flavor and aroma chemicals, agricultural chemicals, and other biologically active specialty products.[1–3] Normally only one enantiomer provides the desired biological activity, yet many reaction schemes used in commercial production yield a racemic mixture. This is inherently inefficient because it limits the maximum attainable yield of active species and thus negatively impacts process productivity and raw material utilization. Furthermore, in some cases unwanted enantiomers can cause undesired side effects when they are included in the final product formulation, so their avoidance or removal may be necessary. A number of separation methods have been developed to isolate a desired active ingredient enantiomer; however, these methods generally are effective only for systems having the required phase behavior, or they may require development of a specific resolving agent such as a specialty extractant, specialized chromatography/adsorption media, or a custom-made membrane. Examples include crystallization,[4] chromatography,[5–8] liquid–liquid extraction,[9,10] and membrane-based separation methods.[11]

Another route to a chiral active ingredient involves production of small molecule chiral synthons (synthetic building blocks) for use as reagents in a subsequent asymmetric (chiral) synthesis.[2,12,13] This approach may be relatively cost effective even if only moderate yield of the chiral synthon can be achieved, because the impact of a relatively low yielding operation on overall cost normally is minimal at an early stage in a multistep process used to produce a final active ingredient; that is, when raw material costs and cumulative processing costs are relatively low. With this in mind, we have focused our efforts toward improving the manufacture of small molecule chiral synthons, and in particular, on making chiral propylene glycol ethers and glycol ether acetates,[14]

Correspondence concerning this article should be addressed to T. C. Frank at tcfrank@dow.com.
Current address of Sol M. Resnick: Calysta Energy, Menlo Park, CA

compounds with potential as synthons for various cardiovascular drugs, antiviral drugs, and chiral crown ethers.[15,16] We used a well-known acylation reaction tactic involving enzyme-catalyzed enantioselective transesterification of a racemic hydroxy compound using an ester as the acyl donor.[17–20] The reaction yields a mixture of (*R*)-enantiomer reaction product and unreacted (*S*)-enantiomer, each with a unique boiling point, so in principle the resulting mixture can be separated by distillation to isolate enantiomers with enhanced chiral purity. Furthermore, we chose to study reversible transesterification with nonactivated esters (nonactivated acyl donors) and the use of reactive distillation to drive conversion. The nonactivated reaction generally is limited by chemical equilibrium such that product or coproduct must be removed from the reaction zone to drive the reaction forward. This is an alternative to the well-established use of activated acyl donors such as vinyl acetate, vinyl butyrate, and isopropenyl acetate. These compounds contain a C═C double bond that allows the acyl donor coproduct to further react in an irreversible manner to drive conversion.[21–23] The reaction can then proceed in a single batch reactor without product removal. An example is the use of vinyl acetate for transesterification, yielding vinyl alcohol that rapidly converts to acetaldehyde. Although commercially successful for select products, the use of activated acyl donors is limited because in certain cases the activated compound can undergo unwanted nonenzymatic side reactions. Another approach termed dynamic kinetic resolution combines enantioselective reaction with racemization of the nonreactive enantiomer.[24,25] This route can produce specific enantiomers of high chiral purity at high yield, but it normally requires developing a dual-catalyst system and not all enantiomers will have a suitably practical racemization pathway.

Thus, we seek to produce chiral synthons via a broadly applicable reactive distillation process scheme using enantioselective acylation with a nonactivated acyl donor and a single catalyst (without racemization). With our model transesterification chemistry, both the substrate and the acyl donor are chiral compounds (supplied as racemates), so the (*R*)-enantioselective reaction can produce four enantiomers with enhanced chiral purity: the two (*R*)-enantiomer reaction products plus the two unreacted (*S*)-enantiomers. The effective overall reaction can be written:

$$(R,S)\text{-A} + (R,S)\text{-B} \leftrightarrow (R)\text{-C} + (R)\text{-D} + (S)\text{-A} + (S)\text{-B} \quad (1)$$

Assuming chemical equilibrium limitations can be overcome and all (*R*)- and (*S*)-enantiomers are of commercial interest, the theoretical conversion of reagents to desired products can approach 100%. To our knowledge, our study is the first to propose this approach for simultaneous production and isolation of four enantiomers. Okasinski and Doherty[26] describe a process for simultaneous production of two enantiomers, (*R*)-propylene glycol and (*S*)-propylene oxide, via cobalt-catalyzed (*R*)-enantioselective reaction of (*R*,*S*)-propylene oxide with water in a single continuous reactive distillation column or by using a closely coupled distillation-column/reactor configuration. Saric, van der Wielen, and Straathof[27] present a theoretical analysis of such systems. We add to this work by introducing a novel horizontal reactive distillation apparatus and a new overall process, and by showing how the use of multiple chiral reagents (supplied as racemates) can increase the number of enantiomers that may be isolated via a single enantioselective reaction scheme.

Reactive Distillation Options for Multicomponent Chiral Resolution

Acylation involves introducing an acyl group (R—C═O) into an organic substrate by reaction with an acylating agent or acyl donor. In many cases, enzyme biocatalysts, particularly lipases, are selective for specific enantiomers and can tolerate nonaqueous environments,[18,28] so the enzyme-catalyzed acylation reaction may be used to generate compounds with enhanced chiral purity. Reactions of this type include transesterification of hydroxy compounds with esters to form the corresponding ester plus coproduct alcohol[20] and reaction of amines with esters to form amides plus coproduct alcohol.[22,29] Similar reactions include transamidation of amines with amides[30] and transamination of ketones with amines.[31,32] As indicated by Reaction 1, the use of chiral compounds (racemates) for both reagents in these kinds of enantioselective reactions presents the prospect for simultaneous production of multiple enantiomers; and, for those reactions that are reversible, *in situ* distillation might be used to drive conversion.

Standard column designs

A typical reactive distillation application is conducted in a vertical distillation column containing trays or packing.[33,34] Well-known examples include the production of methyl acetate from methanol and acetic acid[35–37] and production of methyl *t*-butyl ether from methanol and isobutene.[38] Reactions of this type often are carried out in the presence of an acid catalyst such as homogeneous sulfuric acid or heterogeneous sulfonated ion-exchange beads installed in packets at specific tray or packing locations within the column.

The use of a standard reactive distillation column is feasible only for reactions with sufficiently fast kinetics such that adequate conversion is achieved in the time the liquid spends in the column, which typically is on the order of 5–10 min. Enzyme-catalyzed reactions generally are too slow. Residence time within a column might be increased by using special trays designed to hold a deep layer of liquid,[34] but the vapor must bubble up through the liquid layer at each tray, so vapor-traffic pressure drop must increase in proportion to the height of the liquid layer and the number of trays. This added pressure drop requires that the reboiler operate at a higher pressure and, therefore, a higher temperature, and this can prevent operation within the required temperature range—particularly for applications requiring operation under vacuum at 10 mm Hg (1.3 kPa) or lower to keep temperatures low to minimize catalyst degradation (as in our case). These difficulties may be alleviated by taking the reaction zone out of the column and placing it in one or more separate reaction vessels connected to the column via liquid circulation loops.[26,39,40] The external reactor (or multiple reactors) can then be designed to operate at temperatures that differ from those in the distillation column and with longer liquid-phase residence time. However, this closely coupled reactor-distillation column configuration normally requires sizable additional vessels and heat exchangers that add to the capital and operating costs.

Alternative horizontal designs

Although not well known, a variety of distillation devices with a horizontal configuration have been described in the literature.[41–50] Of these, the most relevant to our work are the horizontal packed distillation apparatus introduced by Dr. Michael Markels, Jr. in the late 1950s[42–44] and the horizontal

esterification reactor/distillation unit introduced by Andrew Spence in 1970.[45,46] The Markels device consists of a horizontal shell divided into compartments containing liquid-irrigated inclined packing for vapor–liquid contacting. The Spence device does not contain packing but uses internal evaporation and condensation heat-transfer zones for countercurrent differential distillation. It is designed for continuous esterification of fatty acids with simultaneous distillation under vacuum to drive conversion. It is an early example of horizontal reactive distillation aimed at enabling the manufacture of polyesters and related condensation polymers.[51]

At Dow in the mid 1980s, Dr. Lanny Robbins introduced another horizontal device as Dow proprietary technology for internal use only—for the purpose of stripping volatiles from sludges and slurries and other feeds that can easily foul standard distillation equipment. We chose this design to use in developing our reactive distillation technology for chiral resolution because of its ability to provide (1) very long liquid-phase residence time needed for our enzymatic reaction (on the order of hours) and (2) very low vapor-traffic pressure drop needed for operation below 10 mm Hg (1.3 kPa). The design concepts and their utility in reactive distillation were disclosed by Dow in 2009.[52] The Robbins design consists of a single horizontal vessel divided into a number of compartments (Figure 1). Unlike the Markels design, no internal packing is used, and there are no internal heat-transfer zones as in the Spence design. The compartments of the horizontal vessel are separated by liquid-traffic baffles. Liquid pumped into the feed compartment (shown on the left-hand side of Figure 1) moves from one compartment to the next through orifices located at the bottom of each baffle. The liquid level in each compartment is easily maintained by using a control valve to adjust the rate at which liquid is removed from the reboiler compartment. In this way, all compartments maintain essentially the same liquid level, and liquid added to the feed compartment must flow toward the reboiler compartment at the opposite end. Vapor moves through the headspace of the vessel in the opposite direction. Within each compartment, vapor and liquid are contacted by circulating liquid to an overhead spray nozzle or splash plate where the liquid is dispersed as droplets falling through the headspace. A high ratio of liquid circulation rate to liquid feed rate may be used to achieve good vapor–liquid contacting for operation near vapor–liquid equilibrium (VLE). Vapor-traffic baffles located in the headspace provide efficient countercurrent contacting of vapor with the spray of liquid droplets that rain down through the headspace. Alternatively, aeration or splash-type mixing impellers may be placed within each compartment to generate drops or sheets of liquid. With this use of spray nozzles, splash plates, or mixing impellers, the headspace of each compartment is operated with the vapor as the continuous phase and the liquid as the dispersed phase. This configuration avoids bubbling vapor through layers of liquid as in a conventional

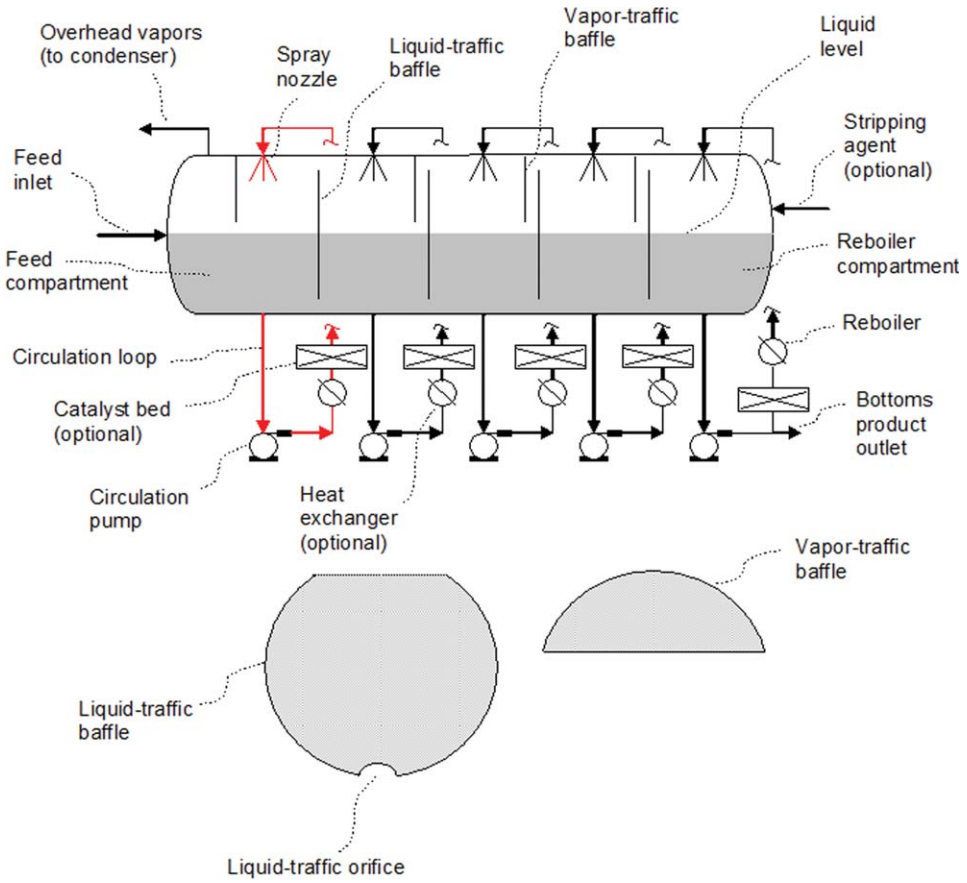

Figure 1. The Robbins horizontal distillation apparatus.

Liquid added to the feed compartment flows through liquid-traffic baffles toward the reboiler compartment where liquid bottoms product is removed. To provide vapor–liquid contacting within each compartment, liquid is circulated through a bottom circulation pump and up to an overhead spray nozzle or splash plate, as highlighted in red.

trayed distillation column, thus avoiding the high vapor-traffic pressure drop that normally would result and permitting the use of large liquid volumes within each compartment to achieve long liquid-phase residence times. Both the Robbins and Markels designs include liquid circulation loops for vapor–liquid contacting; however, the Robbins design uses spray nozzles or splash plates instead of internal packing for a more open design with very low vapor-traffic pressure drop. Catalyst can be placed in fixed beds located within the compartments or within the liquid-circulation lines. Alternatively, a homogeneous catalyst may be dissolved in the feed or injected into any of the compartments.

Model System

Nomenclature

The acronyms, common names, and chemical names of the compounds used in this study are: PnB, propylene glycol *n*-butyl ether, chemical name 1-*n*-butoxy-2-propanol; PnBA, propylene glycol *n*-butyl ether acetate, chemical name 1-*n*-butoxy-2-acetoxypropane; PM, propylene glycol methyl ether, chemical name 1-methoxy-2-propanol; and PMA, propylene glycol methyl ether acetate, chemical name 1-methoxy-2-acetoxypropane.

Vapor pressures and activity coefficients

Maximizing enantioselectivity in our work required operation below 30°C. At this low temperature, the vapor pressure of the reacting mixture is less than 10 mm Hg (1.3 kPa), necessitating distillation under vacuum. Pure component Antoine or Wagner constants are listed in Table 1 along with component molecular weights, liquid densities, and boiling points at atmospheric pressure and at 5 mm Hg (0.67 kPa). This system exhibits nonideal phase equilibrium behavior as indicated by the UNIFAC-derived infinite-dilution activity coefficients listed in Table 2.

Reaction scheme

The equilibrium-limited transesterification reaction that we used to develop the reactive distillation process is written:

$$(R,S)\text{-PnB} + (R,S)\text{-PMA} \leftrightarrow (R)\text{-PnBA} + (R)\text{-PM} + (S)\text{-PnBA} + (S)\text{-PM} \quad (2)$$

However, because the enzyme catalyst is primarily selective for the (*R*)-enantiomers, the amounts of (*S*)-PnBA and (*S*)-PM produced by this reaction will be small. The reaction produces the (*R*)-enantiomer products (*R*)-PnBA and (*R*)-PM and leaves (*S*)-PnB and (*S*)-PMA largely untouched. Thus, at high conversion of (*R*)-PnB (driven by reactive distillation), the reaction mixture will contain mostly (*R*)-PnBA and (*R*)-PM reaction products plus unreacted (*S*)-PnB and (*S*)-PMA (for a feed containing equimolar reagents), and these components can be separated by distillation. Furthermore, this reaction scheme is representative of the general class of acylation reactions for which the acylating agent (PMA in our case) may be used to strip the acylation coproduct (PM) to drive conversion; the acylating agent is higher in molecular weight and, therefore, less volatile, so it can be used to strip the more volatile coproduct from the reaction mixture.

Reaction kinetics and chemical equilibrium

In modeling the reaction kinetics, we began by considering the individual reactions for all possible chiral products:

$$(R)\text{-PnB} + (R)\text{-PMA} \leftrightarrow (R)\text{-PnBA} + (R)\text{-PM} \quad (3)$$

$$(S)\text{-PnB} + (R)\text{-PMA} \leftrightarrow (S)\text{-PnBA} + (R)\text{-PM} \quad (4)$$

$$(R)\text{-PnB} + (S)\text{-PMA} \leftrightarrow (R)\text{-PnBA} + (S)\text{-PM} \quad (5)$$

$$(S)\text{-PnB} + (S)\text{-PMA} \leftrightarrow (S)\text{-PnBA} + (S)\text{-PM} \quad (6)$$

Reaction 3 involves only (*R*)-enantiomers and it dominates the kinetics. The other reactions are much slower but their rates are not necessarily negligible because any reaction producing an (*S*)-enantiomer product will affect the chiral purity of the corresponding (*R*)-enantiomer. To represent chemical equilibrium, the overall equilibrium constant is assumed to be unaffected by the relative amounts of (*R*)- and (*S*)-enantiomers:

Table 1. Liquid Densities, Boiling Points, and Vapor Pressure Correlations

Component	PM	PMA	PnB	PnBA
Molecular weight	90.1	132.2	132.2	174.3
Liquid density at 25°C, in g/mL	0.916	0.963	0.875	0.900
Boiling point at 760 mm·Hg (101.3 kPa), in °C	120.4	146.0	170.0	190.0
Boiling point at 5 mm·Hg (0.67 kPa), in °C	11.1	28.8	48.5	56.5
Parameters for the Extended Antoine Equation and the Wagner Equation (in °C and mm·Hg)				
Component	PM[a]	PMA[a]	PnB[a]	PnBA[b]
C_1	53.92	83.83	83.96	−8.498
C_2	−6812	−8409.6	−9316	0.9635
C_3	0	0	0	−3.755
C_4	0	0	0	−4.695
C_5	−5.017	−9.5943	−9.249	−84.5
C_6	2.263E−18	4.522E−06	6.954E−18	355.6
C_7	6	2	6	
C_8	−96.67	−68.15	−80	
C_9	306.65	324.75	351.75	

Vapor pressures of enantiomers are assumed to be identical.

[a]Extended Antoine Equation: $\ln p_i^* = C_{1i} + \frac{C_{2i}}{T + C_{3i}} + C_{4i}T + C_{5i}\ln T + C_{6i}T^{C_{7i}}$ *for* $C_{8i} \le T \le C_{9i}$.

[b]Wagner Equation: $\ln p_{ri}^* = \left(C_{1i}(1-T_{ri}) + C_{2i}(1-T_{ri})^{1.5} + C_{3i}(1-T_{ri})^3 + C_{4i}(1-T_{ri})^6\right)/T_{ri}$ *for* $C_{5i} \le T \le C_{6i}$

$T_{ri} = T/T_{ci}$

$p_{ri}^* = p_i^*/p_{ci}$

Table 2. Vapor–Liquid Equilibrium at 5 mm·Hg (0.67 kPa)

Component #1	Component #2	Comp #1 Boiling Point at 5 mm Hg (°C)	Comp #2 Boiling Point at 5 mm Hg (°C)	Infinite Dilution Activity Coefficient[a] $\gamma^{\infty}_{1,2}$	Infinite Dilution Activity Coefficient[a] $\gamma^{\infty}_{2,1}$	Inf. Dil. Relative Volatility $\alpha^{\infty}_{1,2}$ $x_1 \to 0$	Inf. Dil. Relative Volatility $\alpha^{\infty}_{2,1}$ $x_2 \to 0$	Azeotrope Formation
PM	PMA	11.1	28.8	1.98	1.96	6.08	0.568	No
PM	PnB	11.1	48.5	1.18	1.27	10.3	0.0844	No
PM	PnBA	11.1	56.5	2.42	2.89	31.4	0.124	No
PMA	PnB	28.8	48.5	1.76	2.02	5.56	0.549	No
PMA	PnBA	28.8	56.5	1.13	1.20	5.49	0.208	No
PnB	PnBA	48.5	56.5	1.78	1.78	2.89	1.11	Yes[b]

[a]Obtained using the UNIFAC correlation available in AspenPlus (version 2006.5 CP5).
[b]An azeotrope is predicted at 5 mm·Hg but not at 200 mm·Hg (27 kPa).

$$K_{eq} = \frac{[\text{PnBA}] \cdot [\text{PM}]}{[\text{PnB}] \cdot [\text{PMA}]} = \frac{\{[(R)\text{PnBA}] + [(S)\text{PnBA}]\} \cdot \{[(R)\text{PM}] + [(S)\text{PM}]\}}{\{[(R)\text{PnB}] + [(S)\text{PnB}]\} \cdot \{[(R)\text{PMA}] + [(S)\text{PMA}]\}} \tag{7}$$

This is consistent with general analyses of molecular chirality that indicate only negligible differences in the Gibbs energies of enantiomers.[53,54]

In developing a kinetic model, we used Langmuir-Hinshelwood kinetic expressions as described by Fogler.[55] For convenience, the model is based on component concentrations instead of activities, as the activity coefficients effectively become incorporated into the empirically derived rate constants and equilibrium constants. Assuming that only one type of active site exists; that is, that activated and nonactivated enzyme sites are equivalent, yields a rate expression of the form

$$\text{rate} = \frac{k_f \cdot [PnB] \cdot [PMA] \cdot x_{cat}}{1 + K'_{ads}[PnB] + K''_{ads}[PMA] + K'''_{ads}[PnBA] + K''''_{ads}[PM]} \cdot \left(1 - \frac{[PnBA] \cdot [PM]}{[PnB] \cdot [PMA] \cdot K_{eq}}\right) \tag{8}$$

The denominator in Eq. 8 accounts for site competition, and each K_{ads} term is specific for the associated species concentration. Analysis of kinetic data indicated that except for PnB, the K_{ads} term is small and can be eliminated. The resulting rate expression depends only on measurable species concentrations, greatly facilitating its development and implementation as compared to more theoretical approaches involving nonmeasureable intermediates such as ping-pong bi bi theory.[56–58]

Equations 9–11 are the rate expressions (in mol/L·min) determined for Reactions 3–5 by analysis of kinetic data. Initial experiments indicated that the rate corresponding to Reaction 6 is essentially zero. The correlation of chemical equilibrium constant as a function of temperature is given by Eq. 12 which indicates that chemical equilibrium does not favor product formation ($K_{eq} = 0.13$ at 30°C), so product or coproduct must be stripped from the reaction mixture to drive conversion.

$$r_3 = \frac{k_3 \cdot \exp\left(\frac{-8142}{1.987}\left(\frac{1}{T} - \frac{1}{297}\right)\right) \cdot [(R)\text{PnB}] \cdot [(R)\text{PMA}] \cdot x_{cat}}{1 + K_{ads} \cdot [(R)\text{PnB}]} \cdot \left(1 - \frac{[\text{PnBA}] \cdot [\text{PM}]}{[\text{PnB}] \cdot [\text{PMA}] \cdot K_{eq}}\right) \tag{9}$$

$$r_4 = \frac{k_4 \cdot \exp\left(\frac{-14{,}000}{1.987}\left(\frac{1}{T} - \frac{1}{297}\right)\right) \cdot [(S)\text{PnB}] \cdot [(R)\text{PMA}] \cdot x_{cat}}{1 + K_{ads} \cdot [(R)\text{PnB}]} \tag{10}$$

$$r_5 = k_5 \cdot \exp\left(\frac{-11{,}811}{1.987}\left(\frac{1}{T} - \frac{1}{297}\right)\right) \cdot [(R)\text{PnB}] \cdot [(S)\text{PMA}] \cdot x_{cat} \tag{11}$$

$$K_{eq} = \exp\left(13.275 - \frac{4653.7}{T}\right) \tag{12}$$

where k_3 = Reaction 3 pre-exponential factor, 1.74E–3 L/[mol·min(mg/mL)]

k_4 = Reaction 4 pre-exponential factor, 1.74E–5 L/[mol·min(mg/mL)]

k_5 = Reaction 5 pre-exponential factor, 5.59E–6 L/[mol·min(mg/mL)]

K_{ads} = equilibrium constant for PnB adsorption, 3.24 L/mol

x_{cat} = enzyme catalyst concentration, mg/mL

T = absolute temperature, Kelvin

Model parameter values were determined by using SIMUSOLV (Trademark of The Dow Chemical Company) software to fit initial-rate data and equilibrium data from batch experiments in Teflon-lined screw top vials (5 mL volume) conducted over a temperature range of 15–45°C. (SIMUSOLV is Dow-developed software used internally at Dow to solve systems of equations). Mixing was provided by rotary shaking at 300 rpm. Samples were taken at 0, 0.25, 0.5, 0.75, 1, 1.5, 2, 4, and 24 h. Total sampling volume was less than 2% of the initial liquid volume, and the effect of this slight volume change was within experimental error. A range of catalyst concentrations was studied, with most data generated using 1.7 mg catalyst beads per mL liquid. Example data for 24°C are shown in Figure 2, and temperature-dependent data are shown in Figure 3. The model fits the data at 24 and 35°C. It underpredicts rates at the more extreme temperatures, but these are outside the process conditions of interest.

Definitions

Chiral purity (% ee)

Enantiomeric excess is defined by

$$\%\,\text{ee} \equiv 100 \times \left|\frac{R-S}{R+S}\right| = |\%R - \%S| \tag{13}$$

In Eq. 13, R and S are the normalized wt fraction (or mol fraction) concentrations of the enantiomers, such that $R + S = 1$. Thus, the % ee number is simply the difference

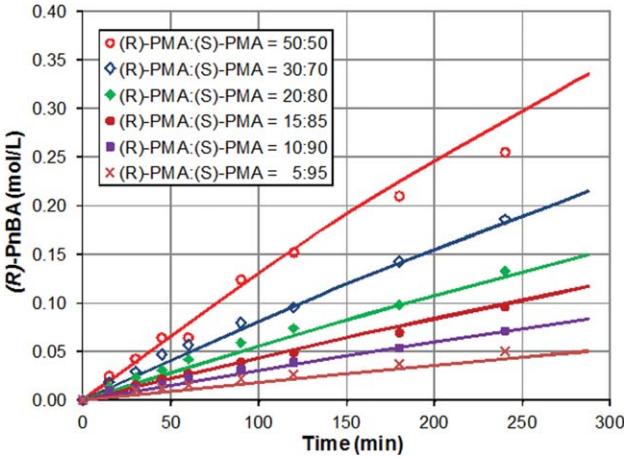

Figure 2. Kinetic model fit for various initial compositions.

Reactions contained PnB and PMA at 50:50 (v/v). Feed compositions (in order from top to bottom in the figure) are (*R*)-PMA:(*S*)-PMA = 50:50 (○); 30:70 (◇); 20:80 (◆); 15:85 (•); 10:90 (■); 5:95 (×). Catalyst was used in the amount of 1.7 mg catalyst beads per mL liquid.

between the normalized concentrations of the two enantiomers.

Conversion

For the continuous steady-state process, conversion is defined as the number of moles of (*R*)-PnB that react per unit time, divided by the number of moles of (*R*)-PnB entering the process in the feed stream per unit time.

Yield

The steady-state flow rate of a specific enantiomer in a product stream (mass or moles per unit time), independent of chiral purity, divided by the maximum theoretical flow rate of that specific enantiomer at 100% (*R*)-PnB conversion and complete separation.

Reactor productivity

The mass of a specific enantiomer, independent of chiral purity, produced per unit volume per unit time. The volume basis is defined as the total liquid-filled volume of the reaction vessel.

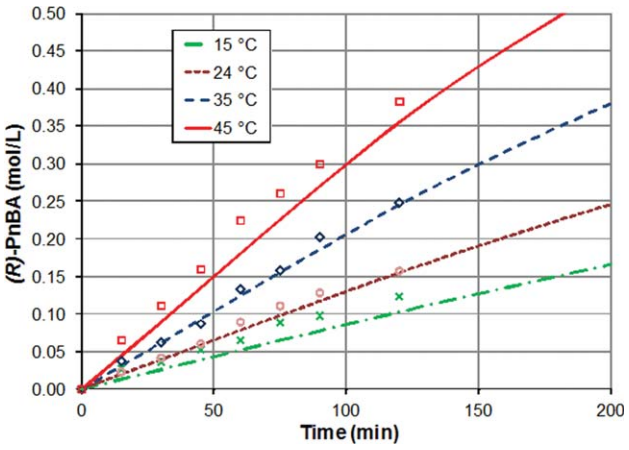

Figure 3. Kinetic model fit for various reaction temperatures.

Lines represent model results. Symbols represent experimental data. Initial reactions contained PnB and PMA at 50:50 (v/v). Catalyst was used in the amount of 1.7 mg catalyst beads per mL liquid.

Recycle ratio

The mass flow rate of material circulating within a recycle loop contained within the overall process, divided by the mass flow rate of total feed entering the process, at steady state.

Residence time

For comparison purposes, we report average liquid-phase residence times calculated from the liquid-filled volume within a single compartment of a multicompartment reactor divided by the average volumetric flow rate of liquid through that compartment at steady state. We chose this way of characterizing residence time as a convenient convention for a given reactor configuration, recognizing that performance is not uniquely determined by total residence time in the reactor; performance depends on the number of compartments (because this affects stripping power) as well as the reactor's total liquid volume and flow rate.

Experimental Materials and Apparatus

Materials

Technical grade racemic PnB and PMA (99+ wt % compound purity) were sourced from Sigma-Aldrich for kinetic experiments and from The Dow Chemical Company for miniplant experiments and were used without further purification.

Enzyme catalyst

The catalyst, a preparation of the enzyme *Candida antarctica* Lipase B immobilized on polyacrylate beads, was obtained from Roche Diagnostics GmbH (Mannheim, Germany), trade name Chirazyme L-2 C2, also known as Novozyme 435. The manufacturer specified the supported enzyme activity to be approximately 10 units/mg. The enzyme used for catalyst preparation was obtained from Biocatalytics (Pasadena, CA).

Analytical methods

An HP (Agilent) 6890 gas chromatograph with flame ionization detector and LEAP-CTC auto-injector was used for analyses. Samples (1.0 μL) were injected at a split ratio of 25:1. The carrier gas was helium at 18–20 psi (constant pressure). Injection port and detector temperatures were 200 and 250°C. A β-DEX 325 chiral column (Supelco, 30 m × 0.25 mm ID, 0.25 μm film thickness) was used to determine enantiopurity and concentration of PnB and PnBA and the enantiopurity of PMA. Baseline separation of PM enantiomers was not achieved using this column. Column temperature was programmed for 70°C with a 0.5 min hold, a 10°C/min ramp to 88°C, and a 20°C/min ramp to 120°C with a 6-min hold. Retention times were: (*R*,*S*)-PM (2.80 min), (*S*)-PMA (4.12 min), (*R*)-PMA (4.24 min), (*S*)-PnB (5.28 min), (*R*)-PnB (5.35 min), (*S*)-PnBA (7.78 min), and (*R*)-PnBA (8.12 min). Racemic samples at 0.25–25 mM in acetonitrile were used for calibration. Internal standard 3-pentanone (20 mM) was added to eliminate injection volume variability. An α-DEX 120 chiral capillary column (Supelco, 30 m × 0.25 mm ID, 0.25 μm film thickness) was used to determine the enantiopurity and concentration of PM and the concentration

of PMA. Column temperature was programmed for 50°C with a 1-min hold, a 7.5°C/min ramp to 75°C, and a 44°C/min ramp to 200°C with a 3 min hold. Racemic PM and PMA in acetonitrile (0.25–25 mM) were used for calibration, giving an $R^2 > 0.99$ for the resolved enantiomers. While baseline separation of (*S*)- and (*R*)-PMA enantiomers was not achieved with this column, the concentration of PMA was determined and could be used to calculate the bulk conversion of PMA to PM. Retention times were: (*S*)-PM (3.68 min), (*R*)-PM (3.82 min), and (*R,S*)-PMA (5.54 min). Prior to analysis, samples were diluted according to 10 μL sample + 490 μL acetonitrile + 100 μL of 120 mM internal standard (3-pentanone).

Miniplant apparatus

The miniplant (Figure 4) consisted of a horizontal stainless-steel vapor chamber connected to six vertical 4-inch (10.2 cm) diameter glass pipes serving as liquid reservoirs, each pipe connected to a liquid circulation loop with an overhead spray nozzle. Note that this design differs somewhat from the full-scale design (Figure 1). In Figure 4, each miniplant compartment is labeled with a compartment number, and the vapor–liquid interface (or liquid level) is located in the lower pipe section (not in the upper vapor chamber) at a position just below the compartment number. This design allows study of the full-scale concept for the horizontal apparatus but in a sufficiently small size for convenient study in the laboratory. That is, the miniplant apparatus was designed to scale down the process concepts illustrated in Figure 1 and mimic operation of a six-compartment vessel at the laboratory scale. The glass pipes provided the needed liquid-phase residence time at the smaller scale, and the vapor chamber provided low vapor-traffic pressure drop to allow operation below 10 mm Hg (1.3 kPa) at temperatures below 30°C.

The vapor chamber was 16 inches (40.6 cm) in diameter and about 60 inches (1.5 m) long including the heads. Each of the interior vapor-space compartments was 8 inches (20.3 cm) wide, separated by internal baffles. These baffles directed the flow of stripping vapor down through a 4-in. (10.2 cm) wide channel and then up and countercurrent to the flow of liquid spray coming from an overhead spray nozzle. The nozzles were obtained from Spraying System Company (Spiral Jet 3/8 HHSJ–SS-90-40, solid cone, 90° spray angle). In each circulation loop, a diaphragm pump was used to pump liquid through a double pipe heat exchanger maintained to control temperature at about 27°C (not shown) into a fixed-bed catalyst holder and then up to the overhead spray nozzle.

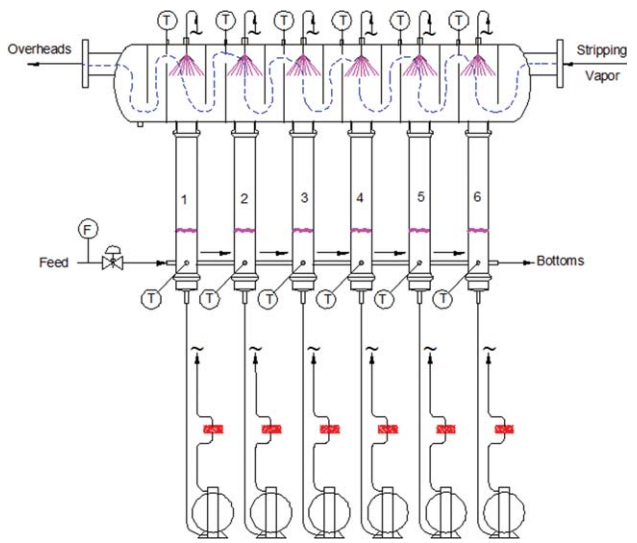

Figure 4. Reactive distillation miniplant.

For each compartment, the main vapor–liquid interface (liquid level) is shown at a position in the pipe section just below the compartment number. Tubing connects adjacent compartments together, allowing liquid to flow from one compartment to the next. Catalyst beds are shown in red.

During operation, a feed stream containing equal amounts of PnB and PMA was continuously fed to the glass pipe shown at the far left-hand side of Figure 4 (compartment 1), and PMA stripping vapor was continuously fed to the vapor chamber at the far right-hand side (compartment 6). A control valve and coriolis mass flowmeter were used to measure and control the liquid feed rate from a nitrogen-pressurized feed tank. Using a similar feed system, PMA liquid was fed to a steam-heated vaporizer coil at a controlled rate to generate stripping vapor. Liquid level in all the compartments was controlled by using a control valve and level probe located at the outlet of compartment 6. The overhead vapor stream from compartment 1 was completely condensed in a chilled condenser. Liquid discharge lines for overheads condensate and bottoms liquid were connected to distillate and bottoms receiver tanks. A CAMILE 3300 laboratory automation system was used for data acquisition and control. Liquid samples were collected using sampling assemblies consisting of a 10 mL metal cylinder connected to a valved manifold (with sample, vacuum, nitrogen, and vent valves) to allow isolation of representative samples during operation.

Process Simulation

The horizontal reactive distillation unit described above was simulated using AspenPlus software, version 2006.5 CP5, as a series of continuous stirred-tank reactors (CSTRs) with countercurrent stripping. Each compartment in the reactive distillation apparatus was modeled as a CSTR using the reaction rate expressions given by Eqs. 9–12 to represent the enzyme-catalyzed reaction (via an Aspen Reactions Subroutine). Thus, for a reactor configuration with six compartments, the simulation included six vapor–liquid contacting stages, each assumed to be in phase equilibrium but not chemical reaction equilibrium—as reaction rates were accounted for by the model rate expressions. All stages were assumed to be at equal pressure. The standard UNIFAC activity coefficient model available in Aspen was used to calculate VLE. Infinite dilution activity coefficients for all binary pairs are listed in Table 2. The solubility of nitrogen gas in the liquid phase was estimated to be less than 40 ppm·mol at 25°C. Estimates were obtained by using the Henry′s Law constant available within Aspen for nitrogen dissolved in ethylene glycol.

Various overall process schemes using the horizontal reactive distillation unit also were simulated in Aspen by using the same kinetic, VLE, and physical property models. These simulations included several additional distillation columns for product isolation and for recycle of stripping agent back to the reactive distillation unit. In all cases, the material and energy balances were solved for the fully integrated process scheme including recycle. Solutions were obtained by using

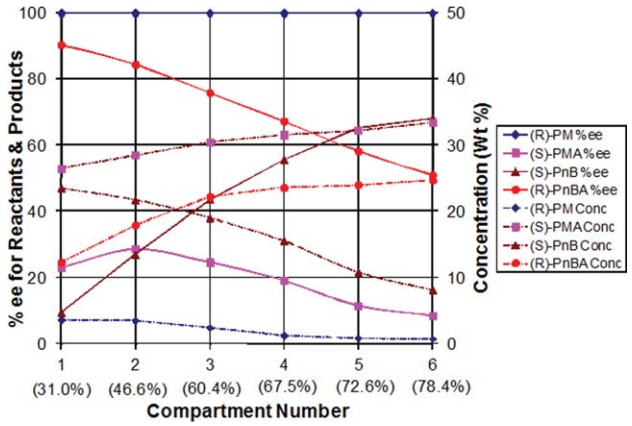

Figure 5. Chiral purities and concentrations of components in the reactive distillation miniplant (actual measured values).

The corresponding level of (*R*)-PnB conversion is indicated in parentheses. Solid lines indicate chiral purity (% ee). Dashed lines indicate component concentrations (wt %).

Broyden and then direct substitution techniques available within Aspen. In solving the material and energy balances for a given process scenario, in some cases the same level of conversion could be obtained by specifying very different amounts of material recycled back to the reactor. The results reported here represent the minimum amount of recycle needed to achieve the specified level of conversion.

Results and Discussion

Miniplant experiments

Figure 5 shows experimental results for a typical miniplant run carried out using vaporized (*R*,*S*)-PMA to strip PM from the reaction mixture in order to produce the two (*R*)-enantiomers. Operating conditions are summarized in Table 3. PMA is less volatile than PM but more volatile than the other components (Table 1), so it can serve to (somewhat) selectively strip PM from the liquid. For these experiments, the PMA used for stripping was introduced as a vapor at the bottoms discharge end of the apparatus (compartment 6 at the right-hand side of Figure 4). Feed containing equal moles of racemic PnB and PMA was introduced to compartment 1 at the other end of the apparatus. The inlet flow rate of racemic PMA stripping vapor was selected to give a stripping factor of roughly 2. The stripping factor is given by the relative volatility of PM with respect to PMA times the ratio of total vapor to total liquid molar flow rates. A value of 2 was chosen in an attempt to insure sufficient stripping performance and avoid operating at an equilibrium-pinched condition. We chose six compartments for these experiments because initial estimates indicated this number would provide a good balance between stripping performance and cost.

As shown in Figure 5, the chiral purity of (*R*)-PnBA varied across the six compartments with increasing conversion, decreasing from 89.9% ee in compartment 1 to 50.9% ee in compartment 6. This is because at higher conversions (*S*)-PnB will compete with (*R*)-PnB in the reaction with (*R*)-PMA to form some (*S*)-PnBA (Reaction 4). As a result, the (*S*)-PnBA concentration increased from 0.62 wt% at the feed compartment (No. 1) to 8.03 wt% in the last compartment (No. 6), as shown in Figure 6. On the other hand, the reactive distillation miniplant produced (*R*)-PM at very high chiral purity (>99.8% ee), because neither the reaction of (*R*)-PnB with (*S*)-PMA (Reaction 5) nor the reaction of (*S*)-PnB with (*S*)-PMA (Reaction 6) proceeds to any significant extent to produce the (*S*)-PM enantiomer under these conditions.

The productivity of the reactive distillation unit is an important measure of its commercial potential. In the miniplant run, the following productivities were achieved for production of the (*R*)-enantiomers (calculated on the basis of liquid-filled vessel volume without product isolation): 35 g/L/h (*R*)-PnBA in the bottoms stream (where the (*R*)-PnBA concentration was 24.5 wt%) and 21 g/L/h (*R*)-PM in the overheads (where the (*R*)-PM concentration was 17.5 wt%, the balance being mostly PMA). This level of productivity compares favorably with those for commercially viable enzymatic chiral resolution processes reported in the literature. For example, we estimate productivity for the membrane-based process described by Lopez and Matson[59] to be on the order of 20 g/L/h (for the isolated product, calculated assuming hollow-fiber membrane modules with 1500 m^2/m^3), and Khmelnitsky et al.[23] report data indicating productivity of roughly 10–20 g/L/h (prior to product isolation) for a single-pot process using an activated acyl donor.

The miniplant run was modeled using the chemical rate expressions and Aspen simulation described earlier. The simulation results were in good agreement with experimental data at moderate conversion levels. The simulation matched experimental concentrations and productivities for the (*R*)-enantiomers quite well, although it underestimated (*S*)-PnBA concentrations at the higher conversion levels (Figure 6). The simulation should provide a reliable assessment of the productivities that can be expected from various overall process schemes. And although (*S*)-enantiomer concentrations are somewhat uncertain at high conversions, the simulation also should provide a reasonable assessment of potential

Table 3. Miniplant Operating Conditions

Pressure	4–5 mm·Hg (about 0.6 kPa)
Temperature	25 to 30°C
Reactor feed rate	2.1 kg/h (40 mL/min)
Stripping vapor feed rate	2.1 kg/h of vaporized (*R*,*S*)-PMA
Bottoms outlet rate	2.3 kg/h
Overheads rate (by material balance)	1.9 kg/h
PMA to PnB ratio in reactor feed	1:1 (mole basis)
Catalyst loading	69 g catalyst beads per compartment
Liquid volume in each compartment	2.6–2.7 L
Total number of compartments	6
Liquid residence time per compartment	1.0–1.2 h
Ratio of circulation rate to reactor feed rate in each compartment	4:1
Total run time	15.5 h (the last 6 h at steady state)

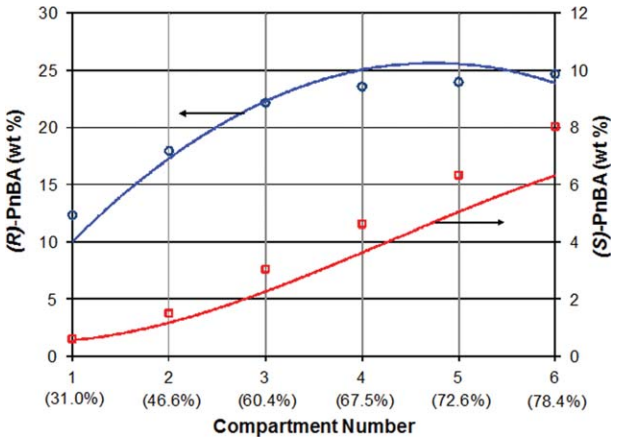

Figure 6. Comparing simulation results with miniplant data.

Lines represent the simulation. Symbols represent experimental data. The corresponding level of (*R*)-PnB conversion is indicated in parentheses.

trends in the chiral purities of the various enantiomers. Thus, the simulation can serve as a useful tool for evaluating potential overall process schemes designed for production of all four enantiomers.

Overall process scheme

The horizontal reactive distillation unit described earlier may be combined with auxiliary product distillation columns in an overall process flowsheet as shown in Figure 7. The process includes a large internal recycle loop (stream 11) that recycles PMA used as stripping vapor in the reactive distillation unit. In evaluating this proposed overall scheme, we used the process simulation program to explore several different options for generating stripping vapor. Material balances corresponding to 90% overall (*R*)-PnB conversion are given in Tables 4–6 for: Option A, *in situ* generation of (*S*)-PMA stripping vapor in a reboiler (Table 4); Option B, external addition of (*R*,*S*)-PMA stripping vapor (Table 5); and Option C, partial recycle of (*S*)-PMA product as

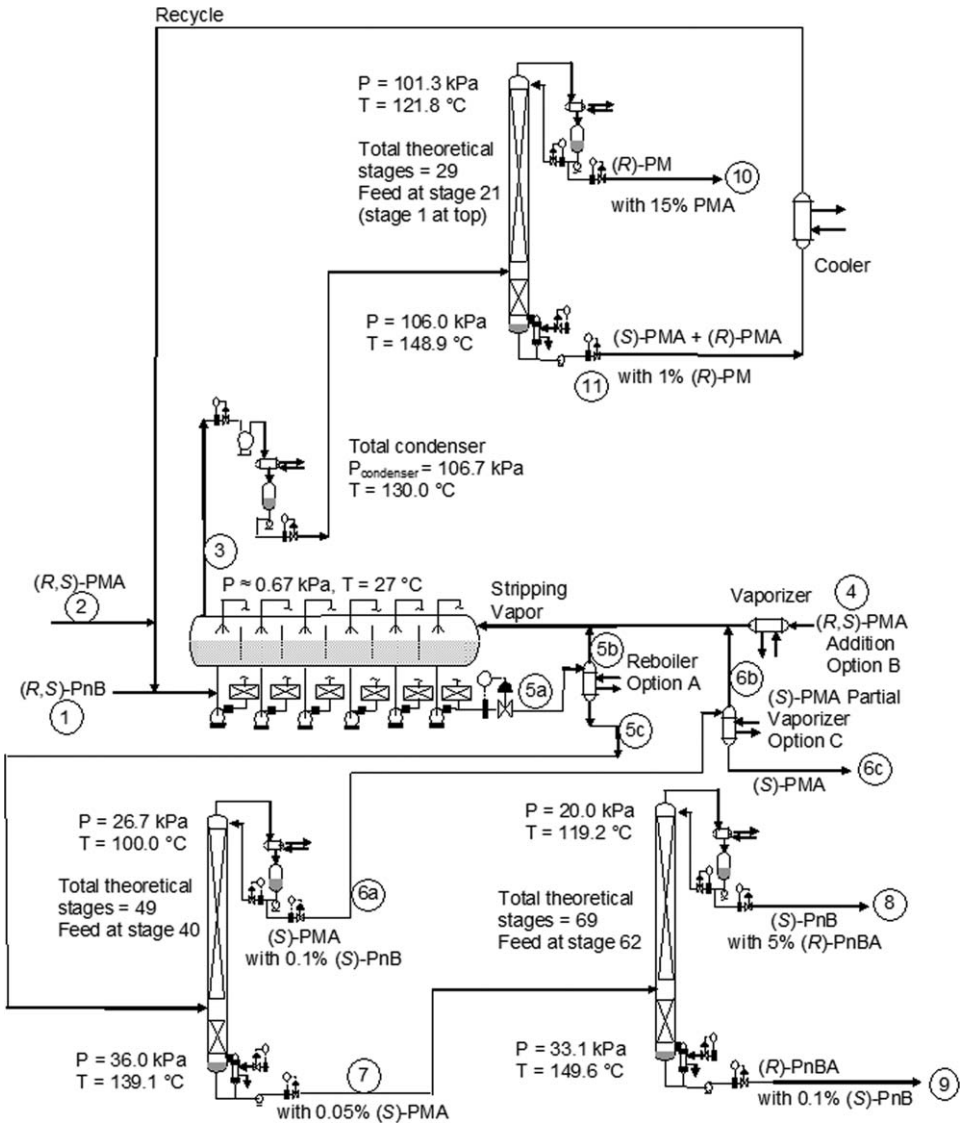

Figure 7. Potential overall process scheme using PMA for stripping: Option A, *in situ* generation of (*S*)-PMA stripping vapor in a reboiler; Option B, external addition of (*R*,*S*)-PMA stripping vapor; and Option C, partial recycle of (*S*)-PMA product as stripping vapor.

See Tables 4–6 for the corresponding material balances.

Table 4. Estimated Material Balance, Chiral Purity, and Productivity for the Process Shown in Figure 7: Option A, *In situ* Generation of (*S*)-PMA Stripping Vapor in a Reboiler

		Composition (wt. fraction) at (*R*)-PnB Conversion = 90%							
Stream No.	Total Flow Rate (kg/h)	(*R*)-PnB	(*S*)-PnB	(*R*)-PMA	(*S*)-PMA	(*R*)-PnBA	(*S*)-PnBA	(*R*)-PM	(*S*)-PM
1	50.0	0.5	0.5	–	–	–	–	–	–
2	50.0	–	–	0.5	0.5	–	–	–	–
3	417.7	0.0464	0.0992	0.2045	0.5669	0.0338	0.0010	0.0458	0.0023
4	0	–	–	–	–	–	–	–	–
5a	212.2	0.0251	0.2392	0.0294	0.4485	0.2289	0.0122	0.0152	0.0015
5b	132.2	0.0214	0.2039	0.0368	0.5622	0.1430	0.0076	0.0228	0.0023
5c	80.0	0.0312	0.2976	0.0171	0.2606	0.3708	0.0198	0.0027	0.0003
6a	22.4	1.05E-4	0.0010	0.0607	0.9276	0	0	0.0096	0.0010
6b	0	–	–	–	–	–	–	–	–
6c					same as 6a				
7	57.6	0.0434	0.4132	0	5.00E-4	0.5154	0.0275	0	0
8	27.7	0.0899	0.8564	6.79E-5	0.0010	0.0500	0.0027	0	0
9	29.8	1.05E-4	0.0010	0	0	0.9483	0.0506	0	0
10	20.0	0	0	0.0541	0.1500	0	0	0.7577	0.0382
11	397.7	0.0488	0.1042	0.2121	0.5879	0.0355	0.0010	0.0100	5.04E-4

	Estimated Chiral Purity of Key Products (% ee)				Potential Reactor Productivity (g/L/h)			
Stream No.	(*R*)-PnBA	(*R*)-PM	(*S*)-PnB	(*S*)-PMA	(*R*)-PnBA	(*R*)-PM	(*S*)-PnB	(*S*)-PMA
6a	–	–	–	87.7	–	–	–	31
8	–	–	81.0	–	–	–	35	–
9	89.9	–	–	–	42	–	–	–
10	–	90.4	–		–	22	–	–

Total Utilities for the Overall Process (kW)	
Heat duty	99.6
Cooling duty	−93.9

Isolated Yield of Products (%)			
(*R*)-PnBA	(*R*)-PM	(*S*)-PnB	(*S*)-PMA
86	89	95	83

Calculations are for a six-compartment horizontal reactive distillation unit operating at 4.35 mm·Hg (0.58 kPa) and 27°C.
Liquid residence time in each compartment: 43.8 min.
Total reactor volume (all six compartments): 678 L.

stripping vapor (Table 6). Thus, in Figure 7, the source of stripping vapor for the reactive distillation unit (from streams 4, 5b, or 6b) depends on which option is specified. For a given option, all vapor streams associated with the other options are set to zero as indicated in Tables 4–6. Another option (Option D) involves use of an inert stripping gas such as nitrogen, as shown in Figure 8 and Table 7. Note that isolated yields of enantiomer products depend on the design of auxiliary separation units as well as overall (*R*)-PnB conversion; in most cases isolated yields exceed 80%. Also note that Figures 7 and 8 are conceptual flow diagrams not intended to show all heat exchangers; total heating and cooling duties calculated in Aspen are given in Tables 4–7. Also, we show a vacuum pump/compressor for generating vacuum and handling overhead vapors and gases in stream 3. This was done for simplicity in simulating the process scheme. More economical vacuum pump and condenser designs could be used for a large-scale, commercial process.

In simulating the process schemes in Figures 7 and 8, a total feed rate of 100 kg/h racemic PnB + racemic PMA feed was chosen as the design basis. Larger production rates, process flows, and equipment sizes are then easily determined by proportion. The molar ratio of reagents entering the overall process in streams 1 and 2 was set at 1:1, which is equivalent to equal mass flow rates of each reagent due to equal molecular weights. We also specified operation at 27°C and 4.35 mm Hg (0.58 kPa) with the same catalyst loading per compartment per unit volume as was used in the miniplant studies (Table 3). At 27°C, the operating temperature was slightly below the maximum allowable temperature for the catalyst (~30°C). Option D allows operation at a somewhat higher pressure while maintaining the same low temperature, if needed, by adjusting the amount of inert gas input to the process. In our work, we chose to consider operation at essentially the same low pressure as for the other options. The stripping vapor leaving the unit in stream 3 is condensed and then fed to an upstream distillation column operating at atmospheric pressure to recover (*R*)-PM and recycle PMA (primarily) back to the horizontal reactive distillation unit. Two downstream distillation columns, each operating under moderate vacuum, are used for separation and recovery of (*S*)-PMA, (*S*)-PnB, and (*R*)-PnBA products. Alternatively, another distillation scheme such as one using a dividing-wall column could be used for this purpose, and cross-exchangers and/or mechanical vapor recompression could be added to reduce overall energy consumption. Also,

Table 5. Estimated Material Balance, Chiral Purity, and Productivity for the Process Shown in Figure 7: Option B, External Addition of (*R*,*S*)-PMA Stripping Vapor

		Composition (wt. fraction) at (*R*)-PnB Conversion = 90 %							
Stream No.	Total Flow Rate (kg/h)	(*R*)-PnB	(*S*)-PnB	(*R*)-PMA	(*S*)-PMA	(*R*)-PnBA	(*S*)-PnBA	(*R*)-PM	(*S*)-PM
1	50.0	0.5	0.5	–	–	–	–	–	–
2	50.0	–	–	0.5	0.5	–	–	–	–
3	705.9	0.0510	0.0948	0.2418	0.5536	0.0275	0.0007	0.0296	0.0010
4	38	–	–	0.5	0.5	–	–	–	–
5a	119.5	0.0208	0.1991	0.1660	0.3385	0.2483	0.0133	0.0137	0.0003
5b	0	–	–	–	–	–	–	–	–
5c				same as 5a					
6a	62.0	1.04E-4	0.0010	0.3197	0.6520	0	0	0.0264	0.0007
6b	0	–	–	–	–	–	–	–	–
6c				same as 6a					
7	57.5	0.0431	0.4126	0	5.00E-4	0.5159	0.0276	0	0
8	27.7	0.0894	0.8564	5.09E-4	0.0010	0.0500	0.0027	0	0
9	29.8	1.04E-4	0.0010	0	0	0.9481	0.0507	0	0
10	18.5	0	0	0.0655	0.1500	0	0	0.7583	0.0261
11	687.4	0.0524	0.0973	0.2465	0.5644	0.0283	0.0007	0.0100	3.45E-4

Stream No.	Estimated Chiral Purity of Key Products (% ee)				Potential Reactor Productivity (g/L/h)			
	(*R*)-PnBA	(*R*)-PM	(*S*)-PnB	(*S*)-PMA	(*R*)-PnBA	(*R*)-PM	(*S*)-PnB	(*S*)-PMA
6a	–	–	–	34.2	–	–	–	105
8	–	–	81.1	–	–	–	62	–
9	89.8	–	–	–	74	–	–	–
10	–	93.3	–		–	37	–	–

Total Utilities for the Overall Process (kW)	
Heat duty	138
Cooling duty	−135

Isolated Yield of Products (%)			
(*R*)-PnBA	(*R*)-PM	(*S*)-PnB	(*S*)-PMA
86	82	95	92

Calculations are for a six-compartment horizontal reactive distillation unit operating at 4.35 mm Hg (0.58 kPa) and 27°C.
Liquid residence time in each compartment: 27.6 min.
Total reactor volume (all 6 compartments): 384 L.

additional separation equipment may be needed to purge from the process any impurities that form due to unintended side reactions.

Note that the horizontal reactive distillation unit is specified to operate with a stripping section only; that is, the distillate vapor is removed at the feed compartment, as shown in Figures 7 and 8. In principle, one might consider adding a rectification section to the horizontal vessel to perform the PM-PMA separation, by adding more compartments and routing feed streams 1 and 2 to a middle compartment, or by adding an ultralow-pressure-drop packed rectification column to the top of the feed compartment. However, rectification is not needed to drive the forward reaction (only stripping is needed), and it is much more practical and less expensive to perform the PM-PMA separation in a separate distillation column that operates at a higher pressure (the column fed by stream 3 in Figures 7 and 8). Furthermore, an auxiliary distillation operation (or some other type of stand-alone separation operation) is necessary to isolate multiple products contained in stream 5.

The various distillation column specifications indicated in Figures 7 and 8 were chosen for a particular design scenario, but these could be adjusted if desired to achieve different compound purities (not chiral purities). The (*R*)-PM recovery column was modeled as a 29-stage distillation column (feed stage at stage 21 from the top) operating at atmospheric pressure. Additional stages could be added to reduce the amount of PMA appearing in the distillate. The downstream columns were specified to operate at 200 mm Hg (27 kPa) and 150 mm Hg (20 kPa) to keep temperatures below 150°C to avoid degrading the (*S*)-PnB and (*R*)-PnBA products. At these conditions, the simulation indicates no azeotropes are formed (Table 2). However, the relative volatility of PnB with respect to PnBA is predicted to be slightly less than 1.1 (at high concentrations of PnB in the overheads), so the PnB/PnBA column design requires a large number of theoretical stages in addition to a high reflux ratio and high reboiler duty (Figure 7 and Table 8). High energy consumption is required to achieve high recovery of (*R*)-PnBA in the bottoms stream (stream 9 in Figures 7 and 8) and to minimize the amount of (*R*)-PnBA in the (*S*)-PnB overheads product (stream 8). Alternatively, to reduce energy consumption the column might be designed to allow a sizable amount of (*R*)-PnBA to contaminate the (*S*)-PnB product in stream 8, and this stream could later be separated using another method; for example, by extracting the more water-soluble component (PnB) into water in a counter-current extraction process.

Table 6. Estimated Material Balance, Chiral Purity, and Productivity for the Process Shown in Figure 7: Option C, Partial Recycle of (*S*)-PMA Product

		Composition (wt. fraction) at (*R*)-PnB Conversion = 90%							
Stream No.	Total Flow Rate (kg/h)	(*R*)-PnB	(*S*)-PnB	(*R*)-PMA	(*S*)-PMA	(*R*)-PnBA	(*S*)-PnBA	(*R*)-PM	(*S*)-PM
1	50.0	0.5	0.5	–	–	–	–	–	–
2	50.0	–	–	0.5	0.5	–	–	–	–
3	374.7	0.0456	0.1003	0.1972	0.5677	0.0353	0.0010	0.0502	0.0025
4	0	–	–	–	–	–	–	–	–
5a	124.7	0.0201	0.1911	0.0330	0.4935	0.2378	0.0127	0.0108	0.0010
5b	0	–	–	–	–	–	–	–	–
5c				same as 5a					
6a	67.2	1.05E-4	0.0010	0.0613	0.9156	0	0	0.0201	0.0018
6b	44.8	8.04E-5	7.66E-4	0.0608	0.9080	0	0	0.0278	0.0025
6c	22.3	1.54E-4	0.0015	0.0623	0.9310	0	0	0.0046	4.25E-4
7	57.5	0.0433	0.4131	0	5.00E-4	0.5155	0.0275	0	0
8	27.7	0.0898	0.8564	6.95E-5	0.0010	0.0500	0.0027	0	0
9	29.8	1.05E-4	0.0010	0	0	0.9483	0.0506	0	0
10	20.1	1.33E-6	0	0.0521	0.1500	0	0	0.7594	0.0384
11	354.6	0.0482	0.1060	0.2055	0.5914	0.0373	0.0011	0.0100	5.06E-4

Stream No.	Estimated Chiral Purity of Key Products (% ee)				Potential Reactor Productivity (g/L/h)			
	(*R*)-PnBA	(*R*)-PM	(*S*)-PnB	(*S*)-PMA	(*R*)-PnBA	(*R*)-PM	(*S*)-PnB	(*S*)-PMA
6c	–	–	–	87.5	–	–	–	31
8	–	–	81.0	–	–	–	35	–
9	89.9	–	–	–	42	–	–	–
10	–	90.4	–		–	23	–	–

Total Utilities for the Overall Process (kW)	
Heat Duty	99.3
Cooling Duty	−94.5

Isolated Yield of Products (%)			
(*R*)-PnBA	(*R*)-PM	(*S*)-PnB	(*S*)-PMA
86	90	95	83

Calculations are for a six-compartment horizontal reactive distillation unit operating at 4.35 mm Hg (0.58 kPa) and 27°C.
Liquid residence time in each compartment: 48.6 min.
Total reactor volume (all 6 compartments): 676 L.

Trade-off between reactor size (residence time) and recycle ratio

One of our goals in developing the simulation was to identify conditions needed to produce enantiomers with enhanced chiral purity near 90% ee. In our initial work (focusing on Figure 7, Option A), we used the simulation to study the effect of liquid-phase residence time on the amount of stripping vapor and thus the stripping power in the reactor and the size of the PMA recycle loop needed to achieve 90% (*R*)-PnB conversion. We found that conversion was increased by increasing the liquid phase residence time and/or the amount of recycle (stripping power), such that process design involved a trade-off between the size of the reactive distillation unit and the size of the recycle loop (Figure 9). For this analysis, we characterized residence time on a per compartment basis for a given multicompartment reactor configuration, and we defined the recycle ratio as the ratio of the recycle mass flow rate (stream 11) to the feed mass flow rate (streams 1 and 2). We also found that at high (*R*)-PnB conversion levels, further increases in conversion increased the chiral purity of the (*S*)-enantiomers at the expense of somewhat reduced chiral purity for the (*R*)-enantiomers (Table 9). Inspection of Eqs. 3–5 indicates that the reduction in (*R*)-PnB and (*R*)-PMA concentrations at higher conversion (yielding higher chiral purity of (*S*)-PnB and (*S*)-PMA products) is accompanied by a small but significant increase in the amount of (*S*)-PnBA and (*S*)-PM produced, and this must reduce the chiral purity of the (*R*)-PnBA and (*R*)-PM even though these products are also increasing in concentration. Although Table 9 details the results for Option A, we expect similar trends for the other options, as well.

Note that for good process flexibility, a given size of horizontal reactive distillation unit may be designed to allow for a range of liquid levels (and thus a range of liquid-phase residence times), and the feed and recycle flows (and thus the recycle ratio) may be adjusted up or down within limits (the recycle flow rate being controlled by changing the amount of stripping vapor generated in the reactive distillation unit′s reboiler or added directly to the process). Thus, residence time and recycle ratio are operating variables that may be adjusted within limits to control (*R*)-PnB conversion and the chiral purity of the various enantiomer products.

Process performance map and operating diagram

To better understand process feasibility and design trade-offs, we devised a process performance map (for a given

Table 7. Estimated Material Balance, Chiral Purity, and Productivity for the Process Shown in Figure 8: Option D, Nitrogen Stripping

Stream No.	Total Flow Rate	Composition (wt. fraction) at (*R*)-PnB Conversion = 90%								
	(kg/h)	(*R*)-PnB	(*S*)-PnB	(*R*)-PMA	(*S*)-PMA	(*R*)-PnBA	(*S*)-PnBA	(*R*)-PM	(*S*)-PM	N_2
1	50.0	0.5	0.5	–	–	–	–	–	–	–
2	50.0	–	–	0.5	0.5	–	–	–	–	–
3a	378.5	0.0424	0.1028	0.1808	0.5815	0.0384	0.0012	0.0484	0.0023	0.0021
3b	377.1	0.0425	0.1031	0.1811	0.5828	0.0386	0.0012	0.0483	0.0023	7.31E-6
4	0.8	–	–	–	–	–	–	–	–	1.0
5	80.3	0.0309	0.2960	0.0176	0.2574	0.3693	0.0197	0.0083	0.0008	0
6	22.8	1.04E-4	0.0010	0.0620	0.9049	0	0	0.0291	0.0028	0
7	57.5	0.0431	0.4131	0	5.00E-4	0.5158	0.0274	0	0	0
8	27.7	0.0895	0.8567	7.11E-5	0.0010	0.0500	0.0027	0	0	0
9	29.8	1.04E-4	0.0010	0	0	0.9484	0.0505	0	0	0
10	19.0	0	0	0.0466	0.1500	0	0	0.7671	0.0362	2.11E-6
11	358.0	0.0448	0.1086	0.1883	0.6058	0.0406	0.0013	0.0100	4.72E-4	0
12	1.5	0.0101	0.0244	0.0800	0.2573	0.0047	1.52E-04	0.0715	0.0034	0.5486

Stream No.	Estimated Chiral Purity of Key Products (% ee)				Potential Reactor Productivity (g/L/h)			
	(*R*)-PnBA	(*R*)-PM	(*S*)-PnB	(*S*)-PMA	(*R*)-PnBA	(*R*)-PM	(*S*)-PnB	(*S*)-PMA
6	–	–	–	87.2	–	–	–	29
8	–	–	81.1	–	–	–	33	–
9	89.9	–	–	–	40	–	–	–
10	–	91.0	–		–	21	–	–

Total Utilities for the Overall Process (kW)	
Heat Duty	88.5
Cooling Duty	−82.8

Isolated Yield of Products (%)			
(*R*)-PnBA	(*R*)-PM	(*S*)-PnB	(*S*)-PMA
86	86	95	83

Calculations are for a six-compartment horizontal reactive distillation unit operating at 4.35 mm Hg (0.58 kPa) and 27°C.
Liquid residence time in each compartment: 58.8 min.
Total reactor volume (all 6 compartments): 714 L.

enantiomer product) showing values of (*R*)-PnB conversion and product chiral purity plotted vs. liquid-phase residence time for a range of recycle ratios. Example maps prepared using the Aspen simulation program are shown in Figure 10 for the process in Figure 7, Option A. Each map shows an increase in conversion with increasing residence time and with increasing recycle ratio. Superimposed on the same map are curves for chiral purity vs. residence time for a range of recycle ratios. The map thus allows the process designer to easily see how conversion and chiral purity are interrelated. For mapping purposes, we chose to focus on conversion instead of yield to characterize the extent of reaction, recognizing that conversion and yield are strongly correlated. The designer can compare the performance maps for the different enantiomers to easily discern what is possible and the trade-offs that are involved. In our example, if we desire 90% (*R*)-PnB conversion and a chiral purity of 90% ee for (*R*)-PnBA, we see from the map that this can be achieved by using a residence time of 0.77 h and a recycle ratio of 4. The map indicates that we could increase the chiral purity of the (*R*)-enantiomers by using a shorter residence time in the reactor, but this would decrease the purity of the (*S*)-enantiomers. Note that the chiral purity of (*R*)-PnBA is not particularly sensitive to recycle ratio at the lower residence times (below about 0.8 h); this is evident in the near convergence of chiral purity curves in this region of Figure 10a. On the other hand, choosing a higher recycle ratio would further improve performance for the (*S*)-enantiomers, but only at the expense of higher operating cost due to the need for larger equipment and higher energy consumption for the recycle loop. For our design, we chose to focus on a residence time of 0.77 h and a recycle ratio of 4 because this yielded good conversion and moderate to high chiral purities without excessive recycle. A quantitative-cost analysis may be conducted using the performance maps as guides to optimize the overall design for a specific set of design goals.

Information contained in the performance maps shown in Figure 10 can be replotted in the form of an operating diagram or design chart to further highlight how the process responds to changes in key operating variables, as shown in Figure 11 for (*R*)-PnBA and (*S*)-PMA. The operating diagram plots operating variables recycle ratio and liquid-phase residence time on the ordinate and abscissa (as in Figure 9), showing how the process responds to changes in these variables during operation by highlighting regions of constant conversion and chiral purity. Figure 11a shows the operating region for obtaining (*R*)-PnBA at 88–91% ee chiral purity, which occurs over a band of (*R*)-PnB conversion levels from about 88–94%. The dashed lines indicating purity were calculated using the minimum recycle ratio needed to achieve the stated purity for a given residence time. Conversion is already fairly high, so each dashed line represents the most

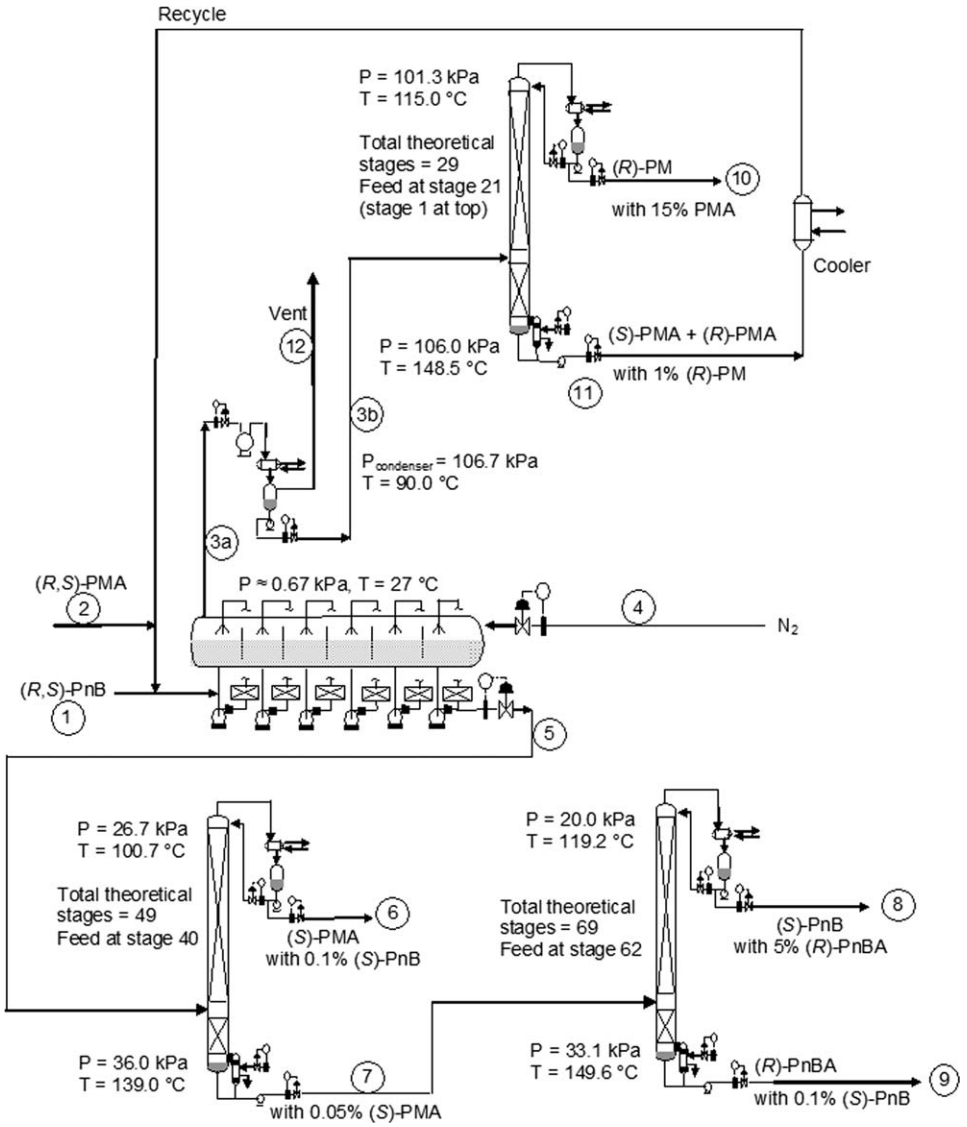

Figure 8. Potential overall process scheme using N_2 for stripping. Option D.

See Table 7 for the material balance.

economical operating region for achieving a desired purity specification with minimum recycle. The resulting diagram may be used as a guide for process adjustment and control strategies. As discussed earlier, (*R*)-PnBA chiral purity is more sensitive to residence time than to recycle ratio, and keeping the residence time below about 0.8 h is critical to achieving high (*R*)-PnBA chiral purity. Similar diagrams and corresponding analysis can be developed for the other enantiomers as well, as shown for (*S*)-PMA in Figure 11b. In this case, (*S*)-PMA chiral purity is shown increasing with increasing residence time.

Comparing options for generating stripping vapor

The use of a reboiler for the horizontal reactive distillation unit (Option A) offers the potential to produce the two (*R*)-enantiomers plus the two (*S*)-enantiomers with a productivity of about 130 g/L/h total product at 90% (*R*)-PnB conversion (Table 4). A reboiler is the usual way of producing stripping vapor for distillation but it is instructive to consider other options as well. Higher reactor productivity may be obtained by using Option B which involves adding racemic PMA vapor directly to the reactor vessel instead of using a reboiler

Table 8. (*S*)-PnB/(*R*)-PnBA Distillation Design Considerations

Case #	(*R*)-PnBA Impurity in (*S*)-PnB Product (%)	(*S*)-PnB Impurity in (*R*)-PnBA Product (%)	Recovery of (*R*)-PnBA (%)	Reflux Ratio	Relative Reboiler Duty
1	1.0	0.1	99.1	13.4	2.73
2	3.0	0.1	97.3	6.0	1.35
3	5.0	0.1	95.3	4.2	1.0

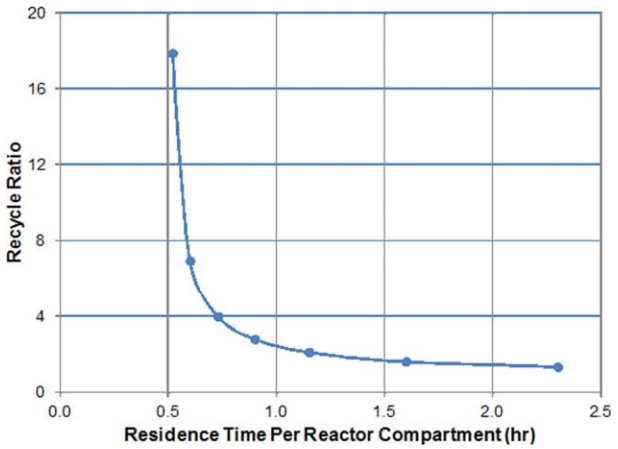

Figure 9. Size of recycle loop (stream 11) vs. liquid-phase residence time per compartment, for 90% (*R*)-PnB conversion (for the process in Figure 7, Option A).

In this analysis, the residence time per compartment was the same for each of the 6 compartments.

(Table 5). Disadvantages include the need to use a higher recycle ratio near 7, a higher demand for utilities, and the inability to produce (*S*)-PMA as an isolated product with high chiral purity. This is because adding (*R*,*S*)-PMA vapor to compartment 6 necessarily will contaminate the liquid with the (*R*)-enantiomer, significantly reducing the chiral purity of (*S*)-PMA in stream 5. However, Option B may be of interest whenever market conditions do not require production of (*S*)-PMA. The higher recycle ratio needed to achieve 90% (*R*)-PnB conversion likely results from the need to handle extra PMA added to the process. By way of comparison, all the other stripping options we consider involve the use of PMA that originates with the feed.

With Option C (Table 6), a portion of the purified (*S*)-PMA product stream is recycled as stripping vapor instead of generating stripping vapor directly in a reboiler. Although Option C is an interesting concept that we initially thought might allow an increase in the chiral purity of the (*S*)-PMA product, it turns out not to offer any significant advantages. At the (*R*)-PnB conversion levels we studied (up to 90%), Option C yields essentially the same performance results as obtained with the use of a reboiler—when compared at the same level of conversion. This is because the relative amounts of (*R*)-PMA and (*S*)-PMA are determined solely by the reaction kinetics and the stripping power achieved within the horizontal reactive distillation unit (as determined by VLE and the vapor to liquid ratio)—and not by the auxiliary downstream distillation units which can only separate non-isomers. There are differences in recycle ratio and stream compositions, but the differences are small as indicated in the tables.

Table 9. Example Chiral Purities as a Function of (*R*)-PnB Conversion[a]

(*R*)-PnB Conversion (%)	Estimated Chiral Purity of Key Products (% ee)			
	(*R*)-PnBA	(*R*)-PM	(*S*)-PnB	(*S*)-PMA
88.0	91.2	91.5	77.7	83.8
89.0	90.6	91.0	79.4	85.8
90.0	89.9	90.4	81.0	87.7
91.0	89.0	89.7	82.6	89.6
92.0	87.8	88.7	84.3	91.5

[a]Basis: Figure 7, Option A

With Option D (Table 7), nitrogen serves as a carrier gas that in our design allows roughly 10% reduction in the demand for utilities. Although reduced, some energy must still be input to the reactor to maintain the reaction temperature. (The required heat exchangers are not shown in Figure 8). The performance results are similar to those for Options A and C; however, they are obtained at the expense of additional costs associated with supplying nitrogen and treating a nitrogen vent stream. Option D may prove more attractive for other potential applications depending on the boiling points and relative volatilities of the various components. The use of an inert gas can allow an increase in operating pressure for a desired operating temperature, if needed. Another potential option involves the use of an inert condensable solvent or entrainer as the stripping medium, ideally something with a boiling point between that of PMA and PM. This option may have merit but the use of a solvent would dilute the reaction and likely reduce productivity. It also would complicate the product distillations, and the solvent′s effect on the catalyst, if any, would need to be taken into account.

In general, with any of these process options, higher productivities may be obtained by increasing the temperature, but at the expense of lower chiral purity because catalyst selectivity is lower at elevated temperatures. Higher productivities also may be obtained by increasing the catalyst loading or the amount of catalyst per unit volume of reactor. Research into new, improved catalysts with higher loadings, higher activity or selectivity, or an ability to tolerate higher temperatures, may yield future improvements in process performance. Reviews of enzymatic and nonenzymatic enantioselective catalysis and catalyst development methods are given elsewhere.[60–65]

Summary and Potential for Future Application

We have proposed a new reactive distillation process involving the use of a horizontal distillation vessel with multiple compartments designed to provide long liquid-phase residence time and low vapor-traffic pressure drop—as an alternative to the use of conventional packed or trayed columns. Experimental data and simulation results for a model (*R*)-enantioselective transesterification reaction [(*R*,*S*)-PnB + (*R*,*S*)-PMA → (*R*)-PnBA and (*R*)-PM reaction products plus unreacted (*S*)-PnB and (*S*)-PMA] show that the process can enable reversible (nonactivated) enantioselective acylation for continuous multicomponent chiral resolution. Distillate and bottoms streams produced by the horizontal vessel can be processed via conventional distillation or another separation method to isolate individual enantiomers and recover stripping media for recycle. The overall process has potential to isolate up to four enantiomers for reactions in which both the substrate and acyl donor are chiral compounds (introduced to the process as racemates). As tools to use in evaluating process feasibility, performance trends, and control strategies, we introduced a process performance map and an operating diagram, each showing substrate conversion and chiral purity as a function of liquid-phase residence time and recycle ratio. These plots facilitate consideration of

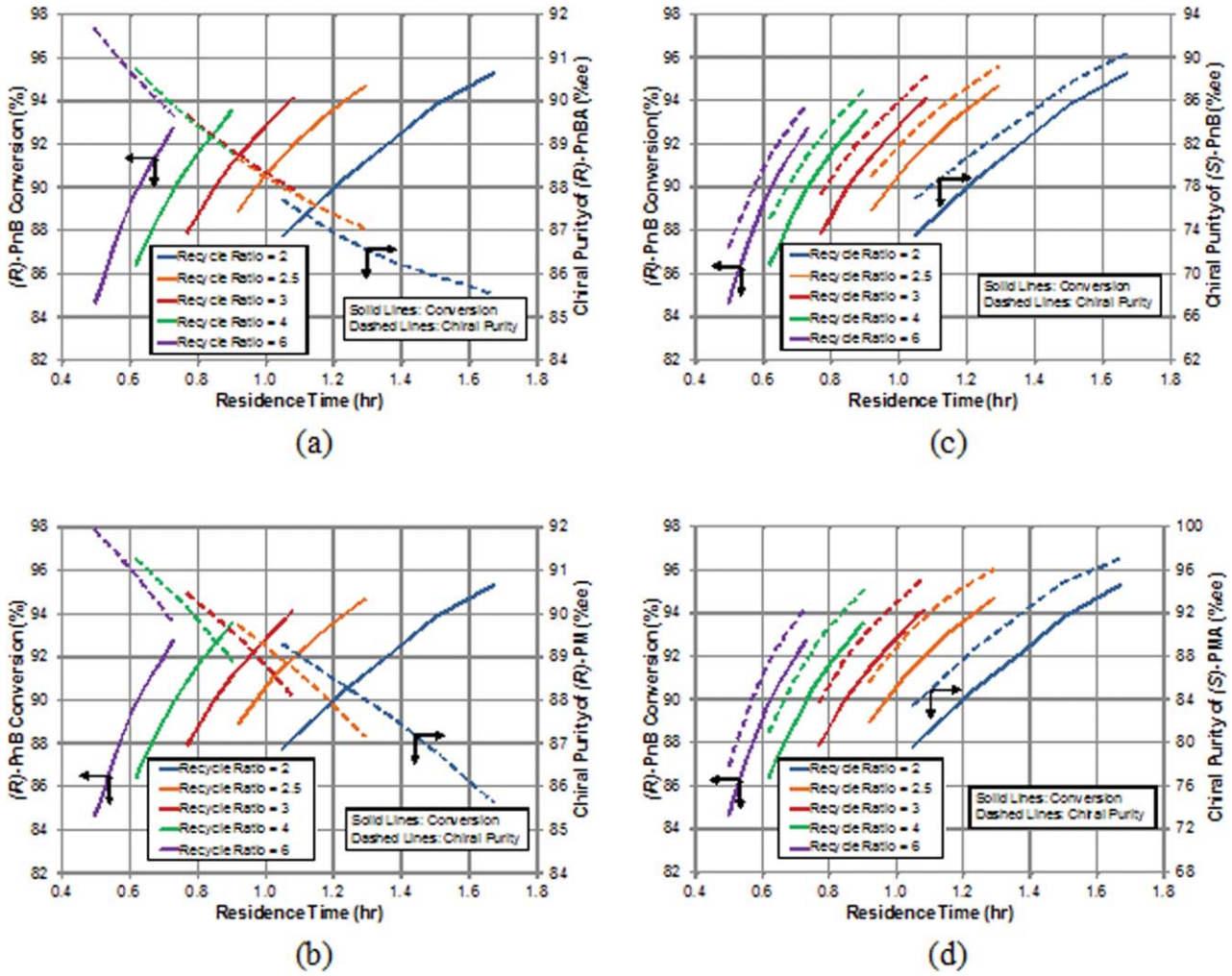

Figure 10. Process performance maps for (a) (*R*)-PnBA, (b) (*R*)-PM, (c) (*S*)-PnB, and (d) (*S*)-PMA, corresponding to Figure 7, Option A.

performance trade-offs involving conversion, chiral purity, reactor size, and stripping power, factors that strongly impact product quality, yield, capital cost, and energy consumption. We also explored various means of producing stripping vapor for the reactive distillation: the use of an internal reboiler; partial vaporization, and reinjection of the nonreactive enantiomer of the acylating agent [(*S*)-PMA in our model reaction]; the use of an inert gas such as nitrogen; and injection of vaporized racemic acylating agent [(*R*,*S*)-PMA]. When applied to our model reaction these options achieve very similar performance results, with the exception that injecting (*R*,*S*)-PMA as stripping vapor allows for higher reactor productivities at the cost of much lower (*S*)-PMA chiral purity.

Our miniplant experiments using the model reaction demonstrated productivity of 56 g/L/h total product at a conversion level of 78% (when producing the two (*R*)-enantiomers), and process simulation indicated that productivities as high as 130 g/L/h total isolated product at 90% conversion may be possible for this system with the current catalyst (when producing all four enantiomers). Potential chiral purities are on the order of 80 to 90% ee, and potential isolated yields for the individual enantiomer products exceed 80%. Specific values vary depending on the specific enantiomer and the details of the process design. Process performance strongly depends on catalyst activity and selectivity, so the proposed process likely will benefit from ongoing catalyst development efforts.

These results suggest that this new reactive distillation process technology has the potential to enable a variety of reversible enantioselective acylations as a means to isolating a broad range of compounds with enhanced chiral purity including various hydroxy compounds, esters, amines, and amides. The technology may be applicable to other equilibrium-limited reactions as well, such a transamidation and transamination. In principle, the enantiomers isolated in this way may be used as synthons in the asymmetric synthesis of various chiral active ingredients for improved production of biologically active products. The technical feasibility of the reactive distillation process will depend upon the suitability of component vapor pressures and VLE for *in situ* distillation at temperatures within the range of viable reaction temperatures, the activity and enantioselectivity of available catalysts, and specifications for chiral purity. Commercial feasibility likely will improve as more highly enantioselective and robust catalysts become available. More broadly, this new approach to conducting reactive distillation may be

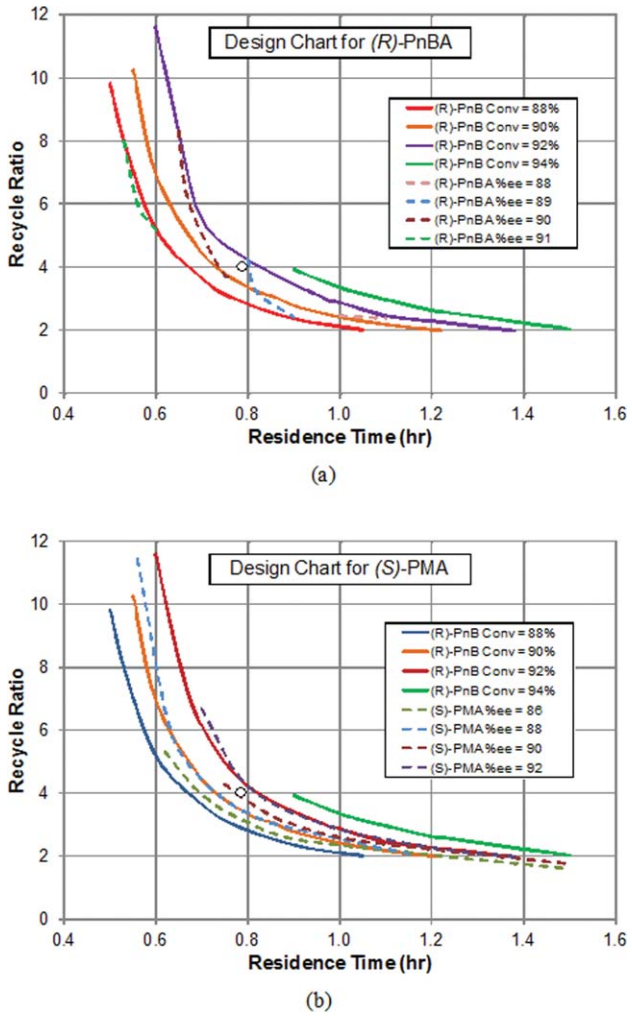

Figure 11. Example operating diagram/design chart for production of (a) (*R*)-PnBA and (b) (*S*)-PMA, in the range of 88–94% PnB conversion.

The white dot shows the operating point for 90% PnB conversion with production of 90% ee (*R*)-PnBA. The dashed lines were obtained by using the minimum recycle ratio needed to achieve the stated purity.

useful for any system requiring long liquid-phase residence time or low vapor-traffic pressure drop.

Acknowledgments

This article describes process research conducted at The Dow Chemical Company mainly during the years 2003–2006. Some more recent analysis also is included. The authors gratefully acknowledge Edward (Ted) Calverley, Herbert Johnson, John Stankowski, and Paul Swanson for valuable discussions of enantioselective reactions and process requirements, and Herbert Johnson and Duane Gibson for help with miniplant design, construction, and operation.

Literature Cited

1. Rekoske JE. Chiral separations. *AIChE J*. 2001;47(1):2–5.
2. Rouhi AM. Chiral chemistry. *Chem Eng News*. 2004;82(24):47–62.
3. Sheldon RA. Chirotechnology: Industrial Synthesis of Optically Active Compounds. New York: Marcel Dekker, 1993.
4. Lorenz H, Perlberg A, Sapoundjiev D, Elsner MP, Seidel-Morgenstern A. Crystallization of enantiomers. *Chem Eng Process*. 2006;45:863–873.
5. Chen X, Yamamoto C, Okamoto Y. Polysaccharide derivatives as useful chiral stationary phases in high-performance liquid chromatography. *Pure Appl Chem*. 2007;79(9):1561–1573.
6. Cox G. Preparative Enantioselective Chromatography. London: Blackwell, 2005.
7. Rajendran A, Paredes G, Mazzotti M. Simulated moving bed chromatography for the separation of enantiomers. *J Chromatogr A*. 2009;1216:709–738.
8. Ribeiro A, Sá Gomes P, Pais L, Rodrigues A. Chiral separation of flurbiprofen enantiomers by preparative and simulated moving bed chromatography. *Chirality*. 2011;23(8):602–611.
9. Jiao FP, Chen XQ, Yang L, Hu YH. Enantioselective extraction of mandelic acid enantiomers using alcohol L-tatrate as chiral selector. *Lat Am Appl Res*. 2008;38(3):249–252.
10. Schuur B, Verkuijl BJV, Minnaard AJ, de Vries JG, Heeres HJ, Feringa BL. Chiral separation by enantioselective liquid-liquid extraction. *Org Biomol Chem*. 2011;9:36–51.
11. Xie R, Chu L-Y, Deng J-G. Membranes and membrane processes for chiral resolution. *Chem Soc Rev*. 2008;37:1243–1263.
12. Christmann M, Bräse S, editors. Asymmetric Synthesis–The Essentials, 2nd ed. Weinheim: Wiley-VCH, 2007.
13. Paquette LA. Handbook of Reagents for Organic Synthesis: Chiral Reagents for Asymmetric Synthesis. Chichester, West Sussex, UK: Wiley, 2003.
14. Resnick SM, Donate FA, Frank TC, Thyne TC, Foley P, inventors; Dow Global Technologies Inc, assignee. Enzymatic resolution of propylene glycol alkyl (or aryl) ethers and ether acetates. US patent 7,264,960. Sept. 4, 2007.
15. Cobley CJ, Holt-Tiffin KE. Asymmetric routes to chiral secondary alcohols. *Pharm Technol*. 2010;S6(suppl):S10–S13.
16. Hoff BH, Waagen V, Anthonsen T. Resolution of 1-phenoxy-, 1-phenylmethoxy-, and 1-(2-phenylethoxy)-2-propanol and their butanoates by hydrolysis with lipase B from Candida Antarctica. *Tetrahedron: Asymmetry*. 1996;7(11):3181–3186.
17. Chen C-S, Sih CJ. General aspects and optimization of enantioselective biocatalysis in organic solvents: the use of lipases. *Angew Chem Int Ed Engl*. 1989;28:695–707.
18. Ghanem A, Aboul-Enein YH. Application of lipases in kinetic resolution of racemates. *Chirality*. 2005:17:1–15.
19. Jacques J, Collet A, Wilen SH. Enantomers, Racemates, and Resolutions. New York: Wiley, 1981.
20. Krishna SH, Persson M, Bornscheuer UT. Enantioselective transesterification of a tertiary alcohol by lipase A from Candida Antarctica. *Tetrahedron: Asymmetry*. 2002:13:2693–2696.
21. Chenevert R, Pelchat N, Morin P. Lipase-mediated enantioselective acylation of alcohols with functionalized vinyl esters: acyl donor tolerance and applications. *Tetrahedron: Asymmetry*. 2009:20:1191–1196.
22. Hanefeld U. Reagents for (ir)reversible enzymatic acylations. *Org Biomol Chem*. 2003;1:2405–2415.
23. Khmelnitsky YL, Michels PC, Cotterill IC, Eissenstat M, Sunku V, Veeramaneni VR, Cittineni H, Kotha GR, Talasani SR, Ramanathan KK, Chitineni VK, Venepalli BR. Biocatalytic resolution of bis-tetrahydrofuran alcohol. *Org Proc Res Dev*. 2011;15(1):279–283.
24. Ahn Y, Ko S-B, Kim M-J, Park J. Racemization catalysts for the dynamic kinetic resolution of alcohols and amines. *Coord Chem Rev*. 2008;252:647–658.
25. Turner NJ. Deracemisation methods. *Curr Opin Chem Biol*. 2010;14:115–121.
26. Okasinski MJ, Doherty MF. Simultaneous kinetic resolution of chiral propylene oxide and propylene glycol in a continuous reactive distillation column. *Chem Eng Sci*. 2003;58:1289–1300.
27. Saric M, van der Wielen LAM, Straathof AJJ. Theoretical performance of countercurrent reactors for production of enantiopure compounds. *Chem Eng Sci*. 2011;66:510–518.
28. Klibanov AM. Improving enzymes by using them in organic solvents. *Nature*. 2001;409:241–246.
29. Balkenhohl F, Ditrich K, Nübling C, inventors; BASF Aktiengesellschaft, assignee. Resolution of racemates of primary and secondary heteroatom-substituted amines by enzyme-catalyzed acylation. US patent 6,214,608. April 10, 2001.
30. Sergeeva MV, Mozhaer VV, Rich JO, Khmelnitsky YL. Lipase-catalyzed transamidation of non-activated amides in organic solvent. *Biotechnol Lett*. 2000;22(17):1419–1422.
31. Tufvesson P, Jensen JS, Kroutil W, Woodley JM. Experimental determination of thermodynamic equilibrium in biocatalytic transamination. *Biotechnol Bioeng*. 2012;109(8):2159–2162.
32. Koszelewski D, Tauber K, Faber K, Kroutil W. ω-Transaminases for the synthesis of non-racemic α-chiral primary amines. *Trends Biotechnol*. 2010;28(6):324–332.

33. Thery R, Meyer X-M, Joulia X. Feasibility analysis, design, and conception of reactive distillation processes: state of the art and critical analysis. *Can J Chem Eng*. 2005;83:242–266 (in French).
34. Towler GP, Frey SJ. Reactive distillation. In: Kulprathipanja S, editor. Reactive Separation Processes, Chapter 2. New York: Taylor & Francis, 2002.
35. Agreda VH, Partin LR, inventors; Eastman Kodak, assignee. Reactive distillation process for the production of methyl acetate. US patent 4,435,595. March 6, 1984.
36. Agreda VH, Partin LR, Heise WH, High-purity methyl acetate via reactive distillation. *Chem Eng Prog*. 1990;86(2):40–46.
37. Huss RS, Chen F, Malone MF, Doherty MF. Reactive distillation for methyl acetate production. *Comput Chem Eng*. 2003;27:1855–1866.
38. Preston KL, inventor; Huntsman Specialty Chemicals Corp, assignee. Use of reactive distillation in the manufacture of methyl t-butyl ether. US patent 5,741,953. April 21, 1998.
39. Gadewar SB, Tao L, Malone MF, Doherty MF. Process alternatives for coupling reaction and distillation. *Chem Eng Res Des*. 2004;82(A2):140–147.
40. Kaymak DB, Luyben WL. Design of distillation columns with external side reactors. *Ind Eng Chem Res*. 2004;43(25):8049–8056.
41. Berly EM, First MW, Silverman L. Recovery of soluble gas and aerosols from air streams. *Ind Eng Chem*. 1954;46(9):1769–1777.
42. Markels M Jr., inventor. Apparatus for horizontal distillation. US patent 2,863,808. Dec. 9, 1958.
43. Markels M Jr., Drew TB. A horizontal fractionating device. *Ind Eng Chem*. 1959;51(5):619–624.
44. Markels M Jr., inventor. Horizontal distillation apparatus. US patent 2,946,726. July 26, 1960.
45. Spence A, inventor; Spence and Green Chemical Co, assignee. Esterification of fatty acids tall oil in a horizontal distillation column and condenser. US patent 3,496,159. Feb. 17, 1970.
46. Spence A, inventor; Spence and Green Chemical Co, assignee. Process for the separation of organic materials by continuous horizontal evaporation and horizontal condensation. US patent 3,496,071. Feb. 17, 1970.
47. Rapier PM, inventor; United States Department of Energy, assignee. Multi-stage flash degasser. US patent 4,346,560. Aug. 31, 1982.
48. Savage K, Wingerson RC, Woodie WL, Wyatt JL, inventors. Mechanically assisted two-phase contactor and fuel ethanol production system. US patent 6,045,660. April 4, 2000.
49. Arrison NL, inventor. Horizontal distillation apparatus and method. US patent application. 2002/0053505 A1. Oct. 18, 2001.
50. Stout TR, inventor. Structure for multiple-effect distillation using tubes or plates. US patent 7,476,298. Jan. 13, 2009.
51. DeBruin BR, inventor; Eastman Chemical Company, assignee. Polyester process using a pipe reactor. US patent 7,541,423. June 2, 2009.
52. IP.com, Inc. Prior Art Database. Horizontal reactive distillation apparatus. Disclosure No. IPCOM000183315D; 4 p. May 18, 2009.
53. Avalos M, Babiano R, Cintas P, Jiménez JL, Palacios JC. From parity to chirality: chemical implications revisited. *Tetrahedron: Asymmetry*. 2000;11:2845–2874.
54. Quack M, Stohner J. Molecular chirality and the fundamental symmetries of physics: influence of parity violation on rovibrational frequencies and thermodynamic properties. *Chirality*. 2003;13(10):745–753. Erratum: Chirality. 2003;15(4):375–376.
55. Fogler HS. Elements of Chemical Reaction Engineering, 4th ed. Englewood Cliffs, New Jersey: Prentice-Hall, 2005.
56. Anthonsen HW, Hoff BH, Anthonsen T. Calculation of enantiomer ratio and equilibrium constants in biocatalytic ping-pong bi-bi resolutions. *Tetrahedron: Asymmetry*. 1996;7(9):2633–2638.
57. Berendsen WR, Lapin A, Reuss M, Non-isothermal lipase-catalyzed kinetic resolution in a packed bed reactor: modeling, simulation and miniplant studies. *Chem Eng Sci*. 2007;62:2375–2385.
58. Kraut J. Serine proteases: structure and mechanism of catalysis. *Annu Rev Biochem*. 1977;46:331–358.
59. Lopez JL, Matson SL. A multiphase/extractive enzyme membrane reactor for production of diltiazem chiral intermediate. *J Membr Sci*. 1997;125:189–211.
60. Seo JS, Lee DWH, Jun SI, Jeon JOYJ, Kim K. A homochiral metal-organic porous material for enantioselective separation and catalysis. *Nature*. 2000;404:982–986.
61. Berglund P. Controlling lipase enantioselectivity for organic synthesis. *Biomol Eng*. 2001;18(1):13–22.
62. Blaser H-U, Pugin B, Spindler F. Progress in enantioselective catalysis assessed from an industrial point of view. *J Mol Catal A: Chem*. 2005;231(1-2):1–20.
63. Pollard DJ, Woodley JM. Biocatalysis for pharmaceutical intermediates: the future is now. *Trends Biotechnol*. 2006;25(2):66–73.
64. Bommarius AS, Blum JK, Abrahamson MJ. Status of protein engineering for biocatalysts: how to design an industrially useful biocatalyst. *Curr Opin Chem Biol*. 2011;15:194–200.
65. Pellissier H. Catalytic non-enzymatic kinetic resolution. *Adv Synth Catal*. 2011;353:1613–1666.

Manuscript received Feb. 23, 2013, and revision received Apr. 26, 2013.